Stress Relaxation in Polymer Melts Following Equibiaxial Step Strain

2 **AUTHORS**, INCLUDING:

David C. Venerus
Illinois Institute of Technology
80 PUBLICATIONS   **1,535** CITATIONS

SEE PROFILE

Macromolecules
ARTICLE

Stress Relaxation in Polymer Melts Following Equibiaxial Step Strain

Teresita Kashyap[†] and David C. Venerus*

Department of Chemical and Biological Engineering and Center of Excellence in Polymer Science and Engineering, Illinois Institute of Technology, Chicago, Illinois 60616. [†]Formerly Teresita Guadarrama-Medina

ABSTRACT: The nonlinear equibiaxial relaxation modulus for two polymer melts, one with linear and one with branched structure, were measured using the technique of lubricated squeezing flow. The experimental technique was validated for Hencky strains up to ~1.6 by demonstrating that results are independent of the lubricant viscosity and thickness. Time−strain factorability of the relaxation modulus was observed for both materials. The measured damping functions were compared with tube model (Doi−Edwards) and pom-pom model (McLeish−Larson) predictions. Damping function data for the linear polymer showed reasonably good agreement with the tube model predictions. The relaxation modulus and the damping function of the branched polymer showed significant differences from the pom-pom model predictions.

Introduction

Stress relaxation following step strain deformation is an experimental protocol that is a widely used to investigate the dynamics of entangled polymer liquids. The dependence of the relaxation modulus (ratio of stress to strain) on time and on strain provide important insights on molecular dynamics. Step shear deformations have been used extensively on polymer melts and solutions, and several reviews are available.[1−3] Step strain flows involving elongational deformations are much more difficult to realize; as a result, experimental data for the flows are rather scarce.

The lubricated squeezing flow (LSF) technique developed originally by Chatraei et al.[4] stands out among other techniques because of its simplicity for generating equibiaxial extensional flow. In recent years, the LSF technique has been evaluated experimentally[5,6] and through modeling[7−9] for constant strain rate and constant stress flows. From these evaluations, lubricant thinning is now understood and as the primary reason the technique is limited to small strains. Methods to overcome this limitation have been under development in recent years.[10,11] On the other hand, LSF is apparently the only technique for stress relaxation experiments following equibiaxial step strain. Research in this area has been focused on the analysis of rheological behavior of polymer melts, but little is known about the limitations of the LSF technique in step strain flow. Table 1 summarizes previous studies where the equibiaxial relaxation modulus, $G_b(\varepsilon_b,t)$, has been measured as a function of Hencky equibiaxial strain, ε_b, for polymer melts. These studies have been done on linear polystyrene (PS) and branched low-density polyethylene (LDPE) melts of various molecular weights, M_w, and polydispersity, M_w/M_n. In all the studies listed in Table 1, time−strain separability of the relaxation modulus $G_b(\varepsilon_b,t) = h_b(\varepsilon_b)G(t)$, where $h_b(\varepsilon_b)$ is the damping function and $G(t)$ is the linear viscoelastic relaxation modulus, was observed.

Experimental data from the studies listed in Table 1 have been used for evaluating rheological constitutive equations. Khan et al.[15] and Khan and Larson[18] examined several differential constitutive equations for linear and branched polymers such as PS, HDPE, and LDPE. The performance of the tube model of Doi and Edwards was first investigated in step equibiaxial flow by

Urakawa et al.[16] for linear polystyrene melts. Isaki et al.[17] and Furuichi et al.[19] examined a modified tube model proposed by Mead, Larson, and Doi; Nishioka et al.[20] studied the well-known K-BKZ equation for linear PS resins. More recently, Okamoto and Yamaguchi[12] analyzed the effect of long branches in a LDPE melt on $G_b(\varepsilon_b,t)$ by comparing experimental data with predictions of the tube model.

The pom-pom model of McLeish and Larson,[21] developed for branched polymers, has been used to describe qualitatively, and in some cases quantitatively, shear and extensional flows.[22−26] However, the applicability of the pom-pom model for equibiaxial step strain flow has yet to be examined.

The remainder of the paper is organized as follows. In the following section, we present the predictions from the well-known tube model and pom-pom model in step equibiaxial deformations. In the third section, we present results from a systematic study of the effect of several experimental parameters on measurements in step equibiaxial deformations using the lubricated squeezing flow technique. In the fourth section, we evaluate the performance of the tube model, both with and without the independent alignment approximation, by comparing predictions of the damping function with our data and other published data on linear polymer melts. We also derive analytic expressions for the equibiaxial relaxation modulus for both the integral and differential versions of the pom-pom model and compare these to the experimental relaxation modulus and damping function for a LDPE melt.

Constitutive Equations

The extra stress tensor for the tube model of Doi and Edwards[27] is given by

$$\boldsymbol{\tau} = \int_{-\infty}^{t} \sum_{i=1}^{N} \frac{g_i}{\tau_i} \exp\left(\frac{-(t-t')}{\tau_i}\right) \mathbf{Q}[\mathbf{E}(t,t')]\, dt' \qquad (1)$$

where τ_i and g_i are the linear relaxation spectra, $\mathbf{Q}[\mathbf{E}(t,t')]$ is the orientation tensor, and $\mathbf{E}(t,t')$ is the deformation gradient tensor. $\mathbf{Q}$ is defined for the rigorous case as $\mathbf{Q} = \langle \mathbf{E}\cdot\mathbf{u}\mathbf{E}\cdot\mathbf{u}/|\mathbf{E}\cdot\mathbf{u}|\rangle/\langle|\mathbf{E}\cdot\mathbf{u}|\rangle$ and for the independent alignment approximation as $\mathbf{Q} = \langle \mathbf{E}\cdot\mathbf{u}\mathbf{E}\cdot\mathbf{u}/|\mathbf{E}\cdot\mathbf{u}|^2\rangle$. Evaluation of eq 1 for a step stain ε_b, in conjunction with the definition of the relaxation modulus, $G_b(\varepsilon_b,t) = \sigma_b/[\exp(2\varepsilon_b) - \exp(-4\varepsilon_b)]$, where $\sigma_b = \tau_{33} - \tau_{11}$, gives the following analytical

Table 1. Summary of Step Equibiaxial Strain Experiments on Melts by Lubricated Squeezing Flow Technique

polymer	name	M_w (kDa)	M_w/M_n	T (°C)	$\varepsilon_{b(max)}$	reference
LDPE	Petrocene 176R	75	3.9	160	1.35	Okamoto et al. (2009)[12]
	LDPE	111	4.8	150	1.5	Nishioka et al. (1998)[13]
	Alathon20	200	8	150	1.23	Soskey and Winter (1985)[14]
	IUPAC A	472	24.9	150	1.4	Khan et al. (1987)[15]
	LDPE1810H	188	11.3	150	1.6	this study
PS	PS606	180	2.5	150	1.35	Urakawa et al. (1995)[16]
	PS F20	189	1.04	160	1.38	Isaki et al. (2003)[17]
	Styron 666	220	2.44	180	1.23	Soskey and Winter (1985)[14]
	PS50 124	250	1.1	160	1.38	Urakawa et al. (1995)[16]
	PSI	398	2.9	161	1.4	Khan et al. (1987)[15]
	PS	423	2.4	160	1.1	Nishioka et al. (1998)[13]
	PS158K	336	2.85	170	1.4	this study
HDPE	HDPE II	152	13	150	1.4	Khan et al. (1987)[15]

expressions for the damping function in equibiaxial step flow[16]

$$h_b(\varepsilon_b)_{\text{RIG}} = \frac{15}{8} \frac{e^{4\varepsilon_b}(e^{6\varepsilon_b}+2)}{(e^{6\varepsilon_b}-1)^2}$$

$$\left(1 - \frac{\sin^{-1}\sqrt{e^{6\varepsilon_b}-1/e^{6\varepsilon_b}}}{\sqrt{e^{6\varepsilon_b}-1}+e^{6\varepsilon_b}\sin^{-1}\sqrt{e^{6\varepsilon_b}-1/e^{6\varepsilon_b}}} \frac{6e^{6\varepsilon_b}}{e^{6\varepsilon_b}+2}\right) \quad (2)$$

$$h_b(\varepsilon_b)_{\text{IA}} = \frac{15}{2} \frac{e^{4\varepsilon_b}}{(e^{6\varepsilon_b}-1)^2}\left(1 - \frac{e^{3\varepsilon_b}}{\sqrt{e^{6\varepsilon_b}-1}}\tanh^{-1}\sqrt{e^{6\varepsilon_b}-1/e^{6\varepsilon_b}}\right)$$
$$+ \frac{5}{2}\frac{e^{4\varepsilon_b}}{e^{6\varepsilon_b}-1} \quad (3)$$

The pom-pom model was derived using ideas from the tube model for a simplified branched molecular structure.[21,28] A pom-pom molecule consists of a backbone which connects two branch points, each having q_i number of arms. In the simplified model, it is assumed that stress arises from the contribution of the backbone alone. The extra stress tensor for the multimode pom-pom model is given by[22]

$$\boldsymbol{\tau}(t) = C\sum_{i=1}^{N} g_i\lambda_i(t)^2 \mathbf{S}_i(t) \quad (4)$$

where $C = 15/4$ for the integral (IPM) and $C = 3$ for the differential (DPM) version of the model. $\lambda_i(t)$ is the backbone stretch ratio, and $\mathbf{S}_i(t)$ the backbone orientation tensor. The evolution equation for $\lambda_i(t)$ with branch-point displacement[23] is governed by

$$\frac{D}{Dt}\lambda_i = \lambda_i\boldsymbol{\kappa} : \mathbf{S}_i - \frac{1}{\tau_{si}}(\lambda_i-1)\exp[\nu_i^*(\lambda_i-1)] \quad (5)$$

where $\boldsymbol{\kappa} = (\nabla\mathbf{v})^T$ is the transpose of the velocity tensor, τ_{si} is the stretch relaxation time of the backbone, and $\nu_i^* = 2/q_i$ is a parameter related to the number of arms. The evolution equation for the backbone orientation tensor for the integral model is

$$\mathbf{S}_i(t) = \int_{-\infty}^{t} \exp\left[\frac{-(t-t')}{\tau_i}\right]\mathbf{Q}[\mathbf{E}(t,t')]\frac{dt'}{\tau_i} \quad (6)$$

The differential approximation for $\mathbf{S}_i$ is defined in terms of a tensor $\mathbf{A}_i$ by

$$\mathbf{S}_i(t) = \frac{\mathbf{A}_i}{\text{tr}[\mathbf{A}_i]} \quad (7)$$

$$\frac{D}{Dt}\mathbf{A}_i - \boldsymbol{\kappa}\cdot\mathbf{A}_i - \mathbf{A}_i\cdot\boldsymbol{\kappa}^T = -\frac{1}{\tau_i}\left(\mathbf{A}_i - \frac{1}{3}\boldsymbol{\delta}\right) \quad (8)$$

The solution of the differential equation for $\mathbf{A}_i$ is given as[29,30]

$$\mathbf{A}_i(t) = \frac{1}{3}\int_{-\infty}^{t} \exp\left[\frac{-(t-t')}{\tau_i}\right]\mathbf{C}(t,t')^{-1}\frac{dt'}{\tau_i} \quad (9)$$

The analytic expressions for the components of $\mathbf{A}_i$ for equibiaxial step strain are

$$A_{11}(t) = \frac{1}{3}[\exp(-t/\tau_i)\exp(-4\varepsilon_b) - \exp(-t/\tau_i) + 1] \quad (10a)$$

$$A_{22}(t) = A_{33}(t)$$
$$= \frac{1}{3}[\exp(-t/\tau_i)\exp(2\varepsilon_b) - \exp(-t/\tau_i) + 1] \quad (10b)$$

For a homogeneous step flow imposed from t_0^- to t_0^+, the solution to eq 5 can be written as

$$\frac{\lambda_i(t_0^+)}{\lambda_i(t_0^-)} = \exp\left[\int_{t_0^-}^{t_0^+} \text{tr}[\boldsymbol{\kappa}(t')^T\cdot\mathbf{S}_i(t')]\,dt'\right] \quad (11)$$

The solution of eq 11 for the differential version of the pom-pom model is given by[29,31]

$$\frac{\lambda_i(t_0^+)}{\lambda_i(t_0^-)} = \sqrt{\frac{\text{tr}[\mathbf{A}_i(t_0^+)]}{\text{tr}[\mathbf{A}_i(t_0^-)]}} \quad (12)$$

The initial stretch ratio for a step equibiaxial strain of magnitude ε_b imposed at $t = 0$ on a relaxed polymer chain is

$$\lambda(0^+,\varepsilon_b) = \sqrt{\frac{1}{3}\exp(-4\varepsilon_b) + \frac{2}{3}\exp(2\varepsilon_b)} \quad \text{differential} \quad (13)$$

For the integral version of the model, the initial stretch ratio can be found by integration of eqs 6 and 11 to give

$$\lambda(0^+,\varepsilon_b) = \exp[\varepsilon_b(Q_{33}-Q_{11})] \quad \text{integral} \quad (14)$$

The components of the Doi–Edwards tensor for the rigorous case are

$$Q_{11} = \frac{\exp(\varepsilon_b)}{4\langle|\mathbf{E}\cdot\mathbf{u}|\rangle}\left[\frac{\exp(-3\varepsilon_b)}{1-\exp(-6\varepsilon_b)}\right.$$
$$\left. + \frac{1-2\exp(-6\varepsilon_b)}{(1-\exp(-6\varepsilon_b))^{3/2}}\sin^{-1}\sqrt{1-\exp(-6\varepsilon_b)}\right] \quad (15a)$$

$$Q_{33} = \frac{1}{2\langle|\mathbf{E}\cdot\mathbf{u}|\rangle}\left[\frac{\sin^{-1}\sqrt{1-\exp(-6\varepsilon_b)}}{\exp(5\varepsilon_b)(1-\exp(-6\varepsilon_b))^{3/2}}\right.$$
$$\left. - \frac{1}{\exp(8\varepsilon_b)(1-\exp(-6\varepsilon_b))}\right] \quad (15b)$$

where

$$\langle |\mathbf{E} \cdot \mathbf{u}| \rangle$$
$$= \left[\frac{1 + \exp(6\varepsilon_b)/\sqrt{\exp(6\varepsilon_b) - 1}\, \sin^{-1} \sqrt{(\exp(6\varepsilon_b) - 1)/\exp(6\varepsilon_b)}}{2 \exp(2\varepsilon_b)} \right]$$
(16)

The backbone stretch, $\lambda_i(\varepsilon_b, t)$, following a step equibiaxial strain is computed by[31]

$$E_1\{v_i^*[\lambda_i(\varepsilon_b, t) - 1]\} - E_1\{v_i^*[\lambda_i(\varepsilon_b, 0^+) - 1]\} = t/\tau_{si} \quad (17)$$

where $E_1(x)$ denotes the exponential integral. Equation 17 is the solution of eq 5 for a homogeneous flow with initial condition $\lambda_i(\varepsilon_b, 0^+)$.

The equibiaxial relaxation modulus for the multimode DPM is given by

$$G_b(\varepsilon_b, t)$$
$$= 3 \sum_{i=1}^{N} g_i \lambda_i(\varepsilon_b, t)^2 \frac{\exp(-t/\tau_i)}{[\exp(-4\varepsilon_b) + 2\exp(-2\varepsilon_b) - 3]\exp(-t/\tau_i) + 3}$$
(18)

and for the IPM by

$$G_b(\varepsilon_b, t) = \frac{15}{4} \sum_{i=1}^{N} g_i \lambda_i(\varepsilon_b, t)^2 \frac{(Q_{33} - Q_{11})\exp(-t/\tau_i)}{\exp(-4\varepsilon_b) - \exp(2\varepsilon_b)} \quad (19)$$

Equations 17 and 18 can not be factorized into strain- and time-dependent functions; hence, in a strict sense, a damping function cannot be computed. To examine the performance of the pom-pom model, experimental damping function will be compared with the ratio $G_b(\varepsilon_b, t)/G(t)$, where $G(t)$ is the linear viscoelastic relaxation modulus.

More recently, Schieber[32] has developed a theory for entangled linear polymers known as the slip-link model. The damping function for the slip-link model in equibiaxial step strains can be expressed in terms of the damping function expressions for the tube model:

$$h_b(\varepsilon_b)_{SL} = \frac{3}{11\langle |\mathbf{E} \cdot \mathbf{u}| \rangle} h_b(\varepsilon_b)_{IA} + \frac{8}{11} h_b(\varepsilon_b)_{RIG} \quad (20)$$

where the damping functions $h_b(\varepsilon_b)_{RIG}$ and $h_b(\varepsilon_b)_{IA}$ are given by eqs 2 and 3, respectively, and $\langle |\mathbf{E} \cdot \mathbf{u}| \rangle$ is given by eq 16.

Experimental Considerations

Materials. Measurements of the stress relaxation after a step equibiaxial deformation were performed on a linear polystyrene (PS158K) and a branched low-density polyethylene (LDPE1810H) by using the LSF technique. The polymers used in this study were from the same batch as those used in previous studies by Hachmann and Meissner,[33] Chodankar et al.,[31] and Guadarrama-Medina et al.[6] The discrete spectrum of relaxation times (τ_i, g_i) obtained from dynamic modulus measurements for LDPE1810H[24] and PS158K[6] are given in Table 2. From these spectra, we calculate the zero shear viscosity $\eta_0 = \sum_i g_i \tau_i$ and mean relaxation time $\tau_p = \sum_i g_i \tau_i^2 / \sum_i g_i \tau_i$. For the LDPE1810H at 150 °C, $\eta_0 = 65$ kPa s and $\tau_p = 80$ s; for PS158K at 170 °C, $\eta_0 = 195$ kPa s and $\tau_p = 75$ s. The nonlinear pom-pom parameters, $q_i = 2/v_i^*$ and τ_i/τ_{si}, shown in Table 2, were determined by Graham et al.[25] using planar elongation data from Hachmann and Meissner.[33] The method for calculating the nonlinear parameters is described by Inkson et al.[22]

Table 2. Relaxation Spectra and Pom-Pom Parameters for LDPE1810H at 150 °C[24] and Relaxation Spectra for PS158K at 170 °C[6]

|	LDPE1810H at 150 °C				PS158K at 170 °C	
i	τ_i (s)	g_i (Pa)	$q_i = 2/v_i^*$	τ_i/τ_{si}	t_i (s)	g_i (Pa)
1	0.002	110471	1	1.0	0.010	87500
2	0.0062	16304	1	1.0	0.032	22000
3	0.019	27180	1	1.0	0.10	34100
4	0.0593	15050	1	1.0	0.32	28400
5	0.184	10613	1	1.0	1.0	19700
6	0.5684	6397.4	1	1.0	3.2	10900
7	1.759	3625.0	1	1.0	10.0	4420
8	5.446	1899.3	1	1.0	31.6	1320
9	16.86	825.84	6	3.0	100	287
10	52.18	300.43	14	1.6		
11	161.5	67.57	16	1.3		
12	500.0	10.58	25	1.0		
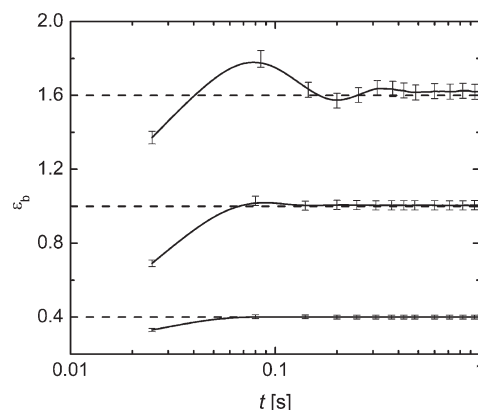
Figure 1. Actual strain versus time for applied Hencky strains of 0.4, 1.0, and 1.6 (bottom to top) with sample LDPE1810H.

Cylindrical samples with 2.5 mm thickness and diameter in the range of 3.2−14.3 mm were prepared by vacuum-compression molding. Silicone oils (GE Viscasil) with viscosities in the range of 0.1−100 Pa s at the test temperatures were used as lubricants. The lubricant to melt viscosity ratio, $\alpha = \mu^L/\eta_0$, was varied over the range 10^{-3}−10^{-7} in this study.

Methods. The equipment used to conduct the step-equibiaxial strain experiments was the RSAIII (TA Instruments). This device uses a direct-drive linear motor capable of imposing deformations up to 3 mm in compression tests. The RSAIII also has a force rebalance transducer (FRT), with a force capacity of 35 N. The transducer was operated in the "FRT" mode (the default setting is "spring mode") to minimize the effects of transducer compliance. Deformations were imposed by changing the total plate separation such that $H/H_0 = [\exp(-2\varepsilon_b) + \phi]/(1 + \phi)$, where $\phi = \delta_0/h_0$ and h_0 and δ_0 are the initial melt half-thickness and lubricant thickness, respectively. Stainless steel plates with $R_p = 7.5$ mm were used in all the experiments. The stress in the melt was calculated from $\sigma_b = F/\pi R^2$, where F is the force exerted on the plate and $R = R_0 \exp(\varepsilon_b)$, the radius of the sample being always less than R_p. Further experimental details can be found in Guadarrama-Medina et al.[6]

In an ideal step strain experiment, the strain is imposed instantaneously. The response time of the RSAIII motor for LDPE 1810H at different strains is shown in Figure 1. For the largest strains, the time required to impose the deformation, t_i, is ∼100 ms. Since $t_i/\tau_p \ll 1$, we assume the finite time to impose the strains has negligible influence on the measured relaxation modulus for $t > 200$ ms. Similar criteria have been suggested by Venerus[2] for shear step strain to avoid artifacts associated with imperfect strain histories. Urakawa et al.[16] and Soskey and Winter[14] reported similar motor response times in step equibiaxial tests.
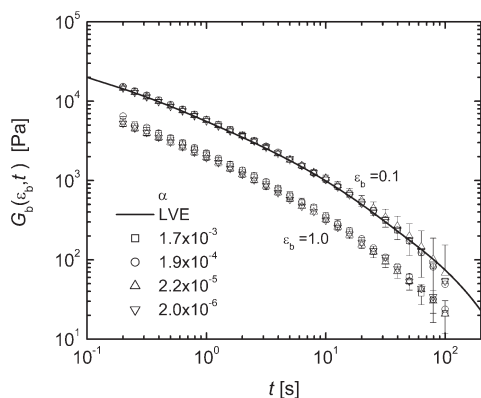
Figure 2. Effect of lubricant viscosity (α) on equibiaxial relaxation modulus for LDPE1810H at 150 °C.
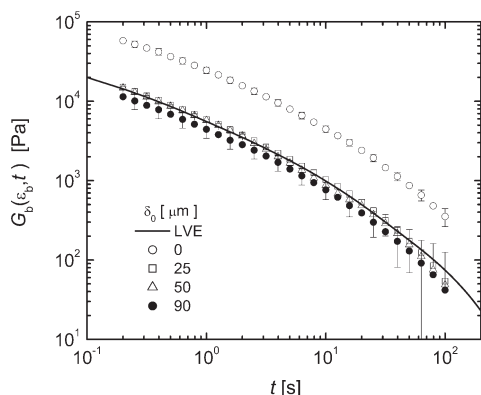

Figure 3. Effect of initial lubricant thickness on the measured equibiaxial relaxation modulus for LDPE 1810H at 150 °C for $\alpha = 1.7 \times 10^{-3}$ and $\varepsilon_b = 0.1$.

The linear viscoelastic relaxation modulus, $G(t) = \sum_{i=1}^{N} g_i \exp(-t/\tau_i)$, was calculated using the relaxation spectra given in Table 2. Since $G(t) = \lim_{\varepsilon_b \to 0} G_b(\varepsilon_b, t)$, comparison with measurements at small Hencky strains provided a useful reference for the LSF technique. All reported data are the average of three repeat experiments; error bars were obtained by propagation of uncertainties in the sample radius ($\pm 10 \ \mu$m), Hencky strain ε_b ($\pm 4\%$), and force (± 0.01 N).

Results and Discussion

Validation of LSF Experiments. We first examine the effect of lubricant viscosity ($\alpha = \mu^L/\eta$) and initial lubricant thickness (δ_0) on the measured equibiaxial relaxation modulus, $G_b(\varepsilon_b, t)$. Figure 2 shows the influence of the lubricant viscosity on $G_b(\varepsilon_b, t)$ over a wide range of α, for LDPE1810H at 150 °C and Hencky strains of 0.1 and 1.0. Results in this figure suggest that the equibiaxial relaxation modulus is independent of lubricant viscosity for α in the range $10^{-3}-10^{-6}$. Similar behavior was observed for PS158K at 170 °C with α in the range $10^{-4}-10^{-7}$ and Hencky strains from 0.1 to 1.4. Soskey and Winter[14] suggested that α of the order of 10^{-3} gives the best lubrication. Figure 3 shows the effect of initial lubricant thickness δ_0 for LDPE 1810H at a strain of 0.1. It appears from this figure that the equibiaxial relaxation modulus is independent of the initial lubricant thickness for δ_0 ranging from 25 to 90 μm. For comparison, this figure also shows unlubricated case $\delta_0 = 0$.

It is interesting to note that the upper limit on Hencky strain in step strain deformations appears to be $\varepsilon_b \leq 1.5$ and independent of polymer type and the instrument used to
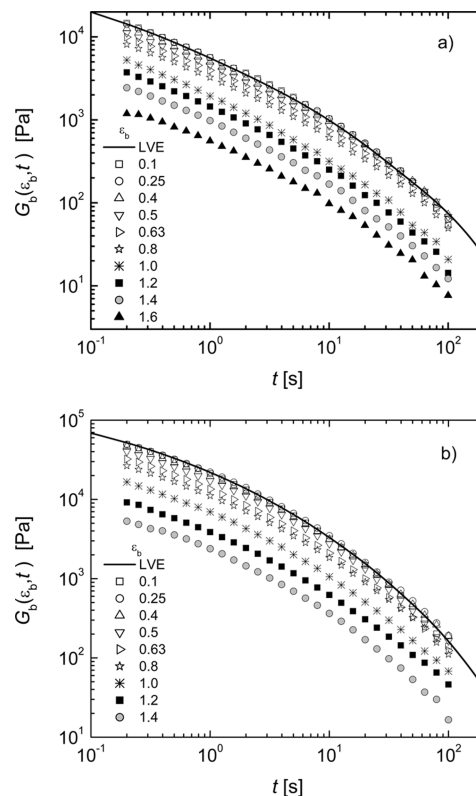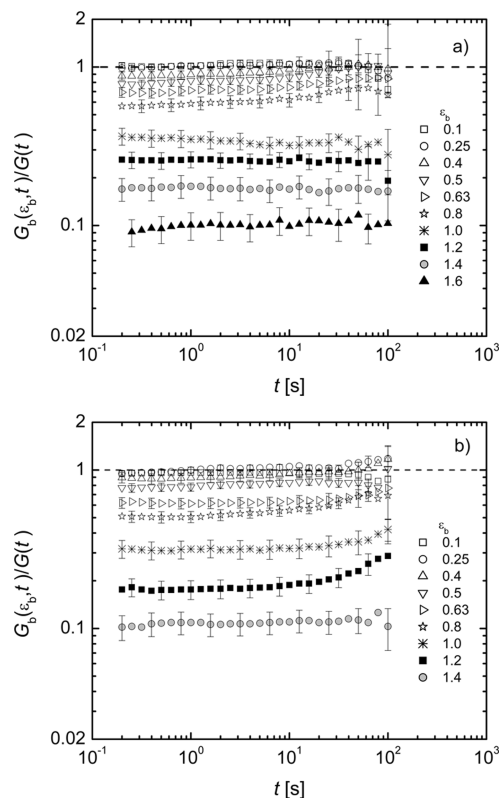

Figure 4. Equibiaxial relaxation modulus versus time for (a) LDPE1810H at 150 °C and (b) PS158K at 170 °C.

conduct the experiment.[12−20] It is also noteworthy that this strain limit is somewhat larger than the upper limit on strain for constant Hencky strain rate experiments, which appears to be $\varepsilon_b \leq 0.5$.[5,6] The most significant difference between the two experiments is that in step strain experiments the stress is measured at constant strain after an "instantaneous" deformation has been imposed, while in constant strain rate experiments, the stress is measured while the sample is undergoing deformation. This difference will have a significant effect on the hydrodynamic behavior of the lubricant film, which has a profound effect on stress measurements in LSF.[6−8] It is also likely that inertial effects in the lubricant film play an important role during the imposition of the deformation in step strain LSF experiments.

Equibiaxial Relaxation Modulus and Damping Function. Experimental $G_b(\varepsilon_b, t)$ results for LDPE1810H and PS158K over a range of Hencky strains are shown in parts a and b of Figure 4, respectively. The modulus for both materials at $\varepsilon_b < 0.5$ follows the linear viscoelastic prediction. These results are in agreement with previous studies by Soskey and Winter,[14] Nishioka et al.,[13] and Okamoto and Yamaguchi.[12] As shown in Figure 4, the maximum strain imposed on LDPE1810H and PS158K was 1.6 and 1.4, respectively, due to the capacity of our force transducer. From the data in these figures it is clear that for each material $G_b(\varepsilon_b, t)$ have the same time dependence and display strain softening; i.e., $G_b(\varepsilon_b, t)$ is a decreasing function of ε_b.

The data in Figure 4 were used to determine the ratio $G_b(\varepsilon_b, t)/G(t)$ shown in Figure 5 for LDPE1810H and PS158K. From this figure, it is evident that this ratio is, within experimental uncertainty, independent of time and that time−strain separability is observed. The average of $G_b(\varepsilon_b, t)/G(t)$ for $1 \ s \leq t \leq 10$ s was used to determine the damping function $h(\varepsilon_b)$. These data are plotted as a function of ε_b for PS158K and LDPE1810H in Figures 6 and 7, respectively, and clearly show pronounced strain softening.

Figure 5. Normalized equibiaxial relaxation modulus versus time for (a) LDPE1810H at 150 °C and (b) PS158K at 170 °C.
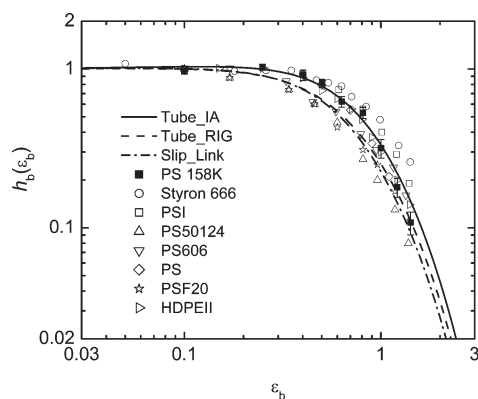
Figure 6. Comparison of experimental damping functions of different linear polymer melts and tube model predictions. Information on the M_w and M_w/M_n for all the melts in this figure is given in Table 1.

Model Predictions and Comparison. Figure 6 shows a comparison of the experimental and predicted damping functions obtained by the tube model for PS158K and published data on other polystyrene melts. It is clear from Figure 6 that $h_b(\varepsilon_b)$ predicted with the tube model is in good agreement with the experimental results. This observation is consistent with the results found in previous investigations.[17,20] Also shown in Figure 6 is the prediction from the slip-link model, eq 20, which is slightly more strain softening than the rigorous version of the tube model. The results in Figure 6 also indicate that $h_b(\varepsilon_b)$ for monodisperse melts with $M_w/M_n \leq 1.1$ (PSF20 from Isaki et al.[17] and PS50124 from Urakawa et al.[16]) are more strain softening than polymers with broad molecular weight distributions and tend to be in better agreement with predictions from the rigorous tube model and slip-link model. It is interesting to note here that in step shear strain flow good agreement between experimental
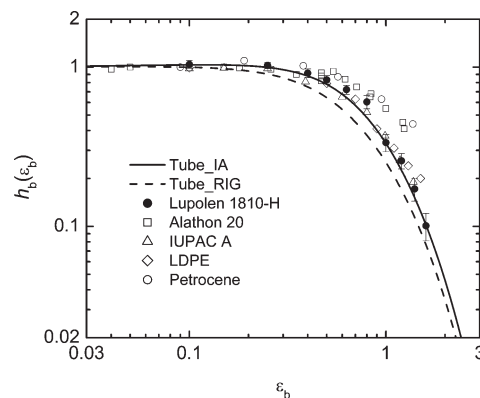
Figure 7. Comparison of experimental damping function of different branched polymer melts and tube model predictions. Information on the M_w and M_w/M_n for all the melts in this figure is given in Table 1.

damping function and tube model predictions is typically observed for monodisperse polystyrene melts and solutions.[1−3]

Figure 7 shows a comparison of the experimental damping functions for five branched polyethylene resins. In this figure, the tube model predictions are used as a reference. It can be observed from Figure 7 that the rigorous tube model agrees reasonably well with data for several polymers (LDPE1810H, IUPAC, and LDPE), but not so well for others (Alathon and Petrocene). In shear flow, the measured damping function for branched polymers is usually larger than that predicted by the tube model.[24,31,34] The observed differences between $h_b(\varepsilon_b)$ data for different LDPE melts may be attributed to the branching structure, or degree of branching, as suggested by Hoyle et al.[26] for step shear strain flow. Indeed, Kirkwood et al.[34] found that the degree of strain softening in the shear damping function was sensitive to branching structure.
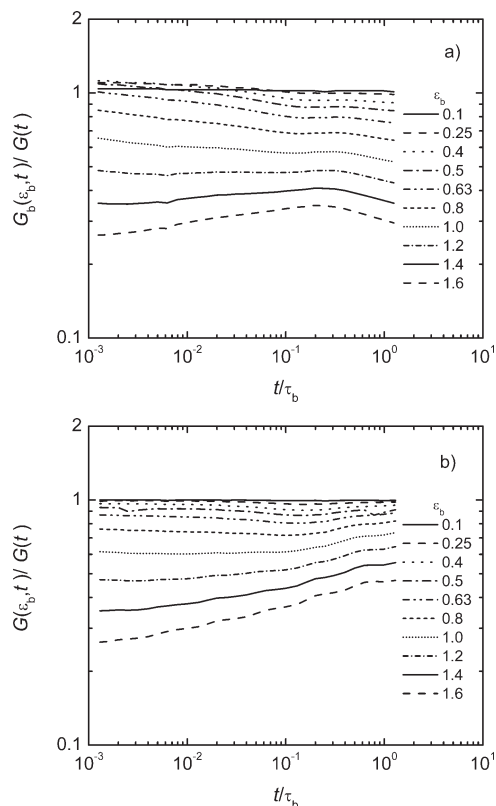
The predictions of the equibiaxial relaxation modulus by the integral (IPM) and differential (DPM) versions of the multimode pom-pom model for LDPE1810H are shown in Figure 8. From this figure we see that the IPM and DPM predictions are qualitatively similar to the experimental data in Figure.4a. Despite the fact that both versions of the pom-pom model do not display time−strain factorability of the equibiaxial relaxation modulus, the damping function was computed from predictions in Figure 8 using the ratio $G_b(\varepsilon_b,t)/G(t)$ at various times.

Figure 9 shows tube model predictions for the ratio $G_b(\varepsilon_b,t)/G(t)$ versus time for the same Hencky strains studied experimentally. The axes chosen in this figure coincide with those in Figure 5a. It is evident from Figure 9 that neither the integral nor the differential form of the model exhibits time−strain separability, as found experimentally in Figure 5a. This observation may be sensitive to the model parameters (τ_{si} and q_i, with i typically running from 1 to 10). Chodankar et al.[31] suggested that by modification of the pom-pom model parameters, ν_i^* and τ_i/τ_{si}, time−strain factorability may be achieved. In a recent study by Hoyle et al.[26] on step shear strain flow, improved time−strain separability was found when $\nu_i^* = 2/(q_i - 1)$, as compared to $\nu^* = 0$ (in this investigation $\nu_i^* = 2/q_i$). In addition, Hoyle et al.[26] observed improved time−strain factorability in predictions computed with 12 modes in the relaxation spectra as compared to 9 modes.

A comparison of the experimental and multimode pom-pom model predictions of the equibiaxial damping function plotted against Hencky strain for LDPE 1810H is shown in Figure 10. The predicted $h_b(\varepsilon_b)$ for both DPM and IPM versions of the model in Figure 10 was obtained from Figure 9, at three different values of t/τ_p, 0.01, 0.1, and 1.0.
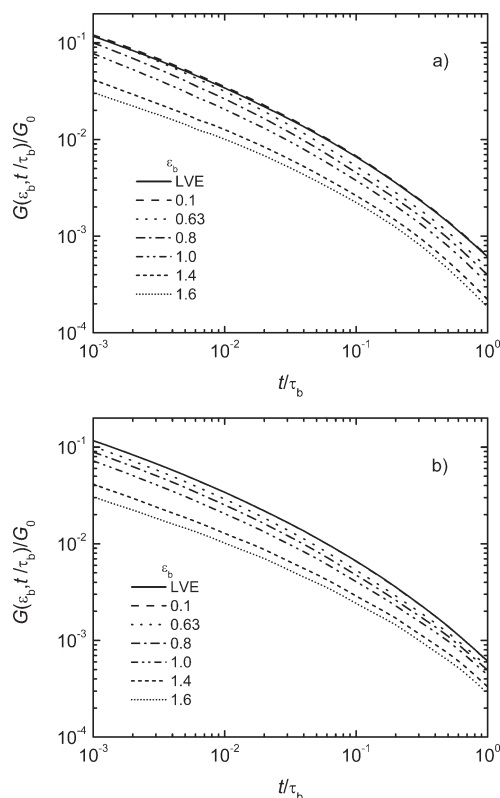
Figure 8. Equibiaxial relaxation modulus predicted by the multimode (a) integral pom-pom model and (b) differential pom-pom model.

Figure 9. Normalized equibiaxial relaxation modulus predicted by the multimode (a) integral pom-pom model and (b) differential pom-pom model.

From this figure, it is evident that the pom-pom model overpredicts the damping function at larger Hencky strains
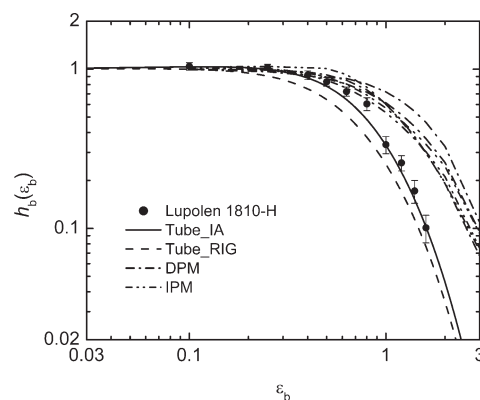
Figure 10. Comparison of experimental and differential (DPM) and integral (IPM) pom-pom model and tube model predictions of the damping function for LDPE1810H.

($\varepsilon_b > 0.8$). The discrepancy observed between experimental values and the IPM and DPM predictions in Figure 10 may be related to the fact that contributions from the arms to the stress are not taken into account in the pom-pom model. In addition, the nonlinear parameters, q_i and τ_{si}, used in the model are obtained by fitting data from planar extensional flow, which is one of the most challenging and least studied flows. Therefore, the accuracy of these parameters should be considered as suggested by Hoyle et al.[26]

Conclusions

The equibiaxial relaxation modulus $G_b(\varepsilon_b,t)$ for a linear polymer (PS158K) and a branched polymer (LDPE1810H) was measured using the lubricated squeezing flow technique. This experimental technique was validated for Hencky strains up to 1.6 by demonstrating that $G_b(\varepsilon_b,t)$ is independent of the lubricant viscosity and lubricant film thickness. Time–strain factorability of the relaxation modulus, $G_b(\varepsilon_b,t) = h_b(\varepsilon_b)G(t)$, was observed for both materials. The measured damping function $h_b(\varepsilon_b)$ was compared with predictions from the tube model (Doi–Edwards) and pom-pom model (McLeish–Larson) and with published data for linear and branch systems. The tube model was found to be in good agreement with experiment values of $h_b(\varepsilon_b)$ for the linear polymers. Good agreement between the predicted damping function from a recently proposed slip-link model was in good agreement with experimental data for linear polymers.

Analytic expressions for the equibiaxial stress relaxation modulus were derived for both the integral and the differential versions of the pom-pom model. Predictions from this model did not display time–strain factorability for the equibiaxial relaxation modulus. Significant discrepancies were observed between the experimental damping function $h_b(\varepsilon_b)$ and that predicted by both versions of the pom-pom model for the branched LDPE1810H, with the experiments showing more strain softening than the models. It is important to note that these pom-pom model predictions were made using parameters obtained from constant rate planar elongation experiments and that predictions using the same parameters were found in previous studies to be in good agreement with shear flow experiments that included step strain, constant strain rate, and exponential strain rate deformations. This result suggests that assumption used in the formulation of tractable versions of the pom-pom model, neglecting the contribution of the arms to stress for example, may need to be reconsidered.

References and Notes

(1) Osaki, K. *Rheol. Acta* **1993**, *32*, 429–437.
(2) Venerus, D. C. *J. Rheol.* **2005**, *49*, 277–295.
(3) Rolon-Garrido, V. H.; Wagner, M. H. *Rheol. Acta* **2009**, *48*, 245–284.
(4) Chatraei, S. H.; Macosko, C. W.; Winter, H. H. *J. Rheol.* **1981**, *25*, 433–443.
(5) Kompani, M.; Venerus, D. C. *Rheol. Acta* **2000**, *39*, 444–451.
(6) Guadarrama-Medina, T.; Shiu, T.-Y.; Venerus, D. C. *Rheol. Acta* **2009**, *48*, 11–17.
(7) Papanastasiou, A. C.; Macosko, C. W.; Scriven, L. E. *Int. J. Numer. Methods Fluids* **1986**, *6*, 819–839.
(8) Venerus, D. C.; Kompani, M.; Bernstein, B. *Rheol. Acta* **2000**, *39*, 574–582.
(9) Burbidge, A. S.; Servais, C. *J. Non-Newtonian Fluid Mech.* **2004**, *124*, 115–127.
(10) Venerus, D. C.; Kompani, M. Apparatus for generating generally uniform compression in viscous liquids. U.S. Patent No. 5,916,599, 1999.
(11) Venerus, D. C.; Shiu, T.-Y.; Kashyap, T.; Hosttetler, J. Submitted to *J. Rheol.*
(12) Okamoto, K.; Yamaguchi, M. *J. Polym. Sci., Part B: Polym. Phys.* **2009**, *47*, 1275–1284.
(13) Nishioka, A.; Takahashi, T.; Masubuchi, Y.; Takimoto, J.; Koyama, K. *Mater. Sci. Res. Int.* **1998**, *4*, 121–123.
(14) Soskey, P. R.; Winter, H. *J. Rheol.* **1985**, *29*, 493–517.
(15) Khan, S. A.; Prud'homme, R. K.; Larson, R. G. *Rheol. Acta* **1987**, *26*, 144–151.
(16) Urakawa, O.; Takahashi, M.; Masuda, T.; Golshan, E. N. *Macromolecules* **1995**, *28*, 7196–7101.
(17) Isaki, T.; Takahashi, M.; Urakawa, O. *J. Rheol.* **2003**, *47*, 1201–1210.
(18) Khan, S. A.; Larson, R. G. *J. Rheol.* **1987**, *31*, 207–234.
(19) Furuichi, K.; Nonomura, C.; Masubuchi, Y.; Ianniruberto, G.; Greco, F.; Marrucci, G. *J. Soc. Rheol. Jpn.* **2007**, *35*, 73–77.
(20) Nishioka, A.; Takahashi, T.; Masubuchi, Y.; Takimoto, J.; Koyama, K. *J. Non-Newtonian Fluid Mech.* **2000**, *89*, 287–301.
(21) McLeish, T. C.; Larson, R. G. *J. Rheol.* **1998**, *42*, 81–110.
(22) Inkson, N. J.; McLeish, T. C. B.; Harlen, O. G.; Grove, D. J. *J. Rheol.* **1999**, *43*, 873–896.
(23) Blackwell, R. J.; Mcleish, T. C. B.; Harlen, O. G. *J. Rheol.* **2000**, *44*, 121–136.
(24) Venerus, D. C. *Rheol. Acta* **2000**, *29*, 71–79.
(25) Graham, R. S.; McLeish, T. C. B.; Harlen, O. G. *J. Rheol.* **2001**, *45*, 275–290.
(26) Hoyle, D. M.; Harlen, O. G.; Ahul, D.; McLeish, T. C. B. *J. Rheol.* **2009**, *53*, 917–942.
(27) Doi, M.; Edwards, S. F. *The Theory of Polymer Dynamics*; Oxford University Press: Oxford, UK, 1986; p 386.
(28) Bishko, G.; Mcleish, T. C. B.; Harlen, O. G.; Larson, R. G. *Phys. Rev. Lett.* **1997**, *79*, 2352–2355.
(29) McKinley, G. H.; Hassager, O. *J. Rheol.* **1999**, *43*, 1195–1212.
(30) Rubio, P.; Wagner, M. H. *J. Rheol.* **1999**, *43*, 1709–1710.
(31) Chodankar, D. C.; Schieber, J. D.; Venerus, D. C. *Rheol. Acta* **2003**, *42*, 123–131.
(32) Schieber, J. D. *J. Chem. Phys.* **2003**, *118*, 5162–5166.
(33) Hachman, P.; Meissner, J. *J. Rheol.* **2003**, *47*, 989–1010.
(34) Kirkwood, K. P.; Leal, L. G.; Vlassopoulos, D.; Driva, P.; Hadjichristidis, N. *Macromolecules* **2009**, *42*, 9592–9608.